Clinical Report

Journal of INTERNATIONAL MEDICAL RESEARCH

Journal of International Medical Research
2017, Vol. 45(6) 2092–2100

DOI: 10.1177/0300060517712164
journals.sagepub.com/home/imr
SAGE

Evaluation of left ventricular strain in patients with dilated cardiomyopathy

Yaohan Yu*, Sisi Yu*, Xuepei Tang, Haibo Ren, Shuhao Li, Qian Zou, Fakui Xiong, Tian Zheng and Lianggeng Gong

Abstract

Objective: Dilated cardiomyopathy (DCM) can cause structural and functional changes in the left ventricle (LV). In this study, we evaluated whether cardiac magnetic resonance tissue-tracking (MR-TT) can be applied to the detection of LV abnormalities in patients with DCM.

Methods: We used MR-TT to analyze the global peak radial strain (GPRS), global peak circumferential strain (GPCS), and global peak longitudinal strain (GPLS) in every segment of the LV in 23 patients with DCM and 25 controls. The LV ejection fraction was also measured as a function indicator.

Results: Compared with the controls, the GPRS, GPCS, and GPLS were significantly reduced in patients with DCM, indicating global LV function impairment in all directions. We also identified a significant linear correlation between the GPRS, GPCS, and GPLS and the LV ejection fraction, indicating that LV function relies on coordinated wall motion from all directions. Moreover, we found that patients with DCM had a significantly reduced magnitude of the PRS, PCS, and PLS in most segments at different levels, indicating impaired myocardial function in most LV regions.

Conclusions: Our results demonstrate that LV myocardial strain in patients with DCM can be sensitively detected by MR-TT (not only the global LV function changes but also the segmental strain), which can help to identify the injured segment at an early stage and guide clinical treatment.

Keywords

Dilated cardiomyopathy, tissue tracking, cardiac magnetic resonance imaging, myocardial strain

Date received: 15 December 2016; accepted: 3 May 2017

Introduction

Dilated cardiomyopathy (DCM) is the third leading cause of heart failure. It accounts for 30% to 40% of cases of heart failure, with a prevalence of 36 patients per 100,000 population. Every year, 5 to 8 new DCM cases are diagnosed per 100,000 persons, and 10,000

Department of MRI, The Second Affiliated Hospital of Nanchang University, 1 Minde Road, Nanchang, Jiangxi, China

*These authors contributed equally to this work.

Corresponding author:
Lianggeng Gong, Department of MRI, The Second Affiliated Hospital of Nanchang University, 1 Minde Road, Nanchang, Jiangxi 330006, China.
Email: GongLianggeng@gmail.com

patients lose their lives.[1,2] DCM is characterized by an enlarged and weakened left ventricle (LV) in the absence of heavy loading conditions (e.g., hypertension, valve disease) or ischemic heart disease sufficient to cause global systolic impairment.[2] Therefore, the use of sensitive techniques to detect deregulated LV myocardial function would be of immense value for early diagnosis and assessment of the therapeutic effect in patients with DCM.

In the clinical setting, myocardial strain is a sensitive measurement of the fiber length change during ventricle contraction; it has therefore been used to determine LV myocardial mechanical function and deformation in patients with DCM. In the past, cardiac magnetic resonance (MR) tagging was a reference standard technique for the assessment of myocardial strain, including harmonic phase analysis and spatial modulation of magnetization.[3] However, MR-tagging requires a specific image acquisition scheme and dedicated software as well as tedious and time-consuming manual analysis, which preclude its routine clinical use.[4] Speckle-tracking echocardiography technology has also been recently used to analyze the LV myocardial strain. However, the reliability and accuracy of speckle-tracking echocardiography largely depends on image quality. Poor image usually results in drift or incorrect calculation.[5] In recent years, cardiac MR imaging (CMR) has become a reliable and accurate modality for quantification of global LV function with high spatial and temporal resolution.[6] Cardiac MR tissue-tracking (MR-TT) technology makes use of tissue voxel motion tracking on steady-state free precession images; therefore, it inherently has less variation in the myocardial tissue signals when measuring longitudinal, circumferential, and radial LV strains.[7] MR-TT is also rapid and semiautomative, requiring no additional scans or sequences, and has a shorter post-processing time than traditional MR-tagging.[4] Moreover, MR-TT has high spatial and temporal resolution, which is more accurate than speckle-tracking echocardiography.[8]

Therefore, in the current study, we used MR-TT to measure LV global and regional strain in patients with DCM and studied the correlation between different peak strains.

Patients and methods

Study population

All procedures in the present study were performed with the approval of the institutional review board and ethics committee of the Second Affiliated Hospital of Nanchang University and in accordance with the 1964 Helsinki declaration. Written informed consent was obtained from all participating individuals prior to the study. We prospectively recruited 23 consecutive patients who had been referred for CMR from 2012 to 2015 after a clinical diagnosis of DCM at the Second Affiliated Hospital of Nanchang University. The diagnosis of DCM was based on the 1995 World Health Organization/International Society and Federation of Cardiology criteria.[9] All patients with DCM had impaired systolic function (LV ejection fraction [LVEF] of $<50\%$). Patients with significant coronary artery disease, valvular disease, hypertensive heart disease, and congenital abnormalities were excluded. All patients were examined in a clinically stable condition (New York Heart Association functional class of <III). Twenty-five healthy volunteers were also recruited based on the following criteria: (i) no symptoms of cardiovascular dysfunction, (ii) normal cardiac morphology and function as proven by CMR, and (iii) no history of inflammatory disease including the common cold virus in the most recent 2 weeks before examination.

CMR acquisition

All CMR examinations were performed on 1.5 T and 3.0 T scanners (GE Signa Excite HD Twinspeed), with a maximum gradient strength of 33 mT/m and a slew rate of 120 mT/m/s. An 8-channel phased-array coil was used for signal reception, and vector electrocardiography was used for cardiac gating. Electrocardiogram-gated steady-state free precession cine sequences were acquired during brief periods of breath-holding in 12- to 13-s equidistant short-axis planes (Axi) completely covering the LV. The parameters of steady-state free precession were as follows: 8-mm thickness, 1- to 2-mm gap, 360×320 mm field of view, and 140×140 matrix size. Long-axis images (apical four-chamber [4-ch] and two-chamber [2-ch]) were used for subsequent analysis.

Tissue-tracking imaging

CMR tissue-tracking (CMR-TT) post-processing software (cvi42 & Tissue Tracking; Circle Cardiovascular Imaging, Alberta, Canada) was used to analyze the LV strain, Axi view, and 4- and 2-ch views of the ventricle, which were divided according to the American Heart Association (AHA) 17-segment model. The apical cap (segment 17) was not considered for analysis. This tool includes a software-based feature-tracking algorithm that has been previously validated in experimental and clinical studies. These previous studies confirmed that the software has good agreement and reproducibility.[7] We drew the endocardial and epicardial borders from the short-axis, 4-ch, and 2-ch views at end-diastole and end-systole; the papillary muscles were excluded from the endocardial contour. The longitudinal, circumferential, and radial strain values were obtained. The global graph and bull's eye diagram of AHA are shown in Figure 1. The global and regional strain in the LV were respectively analyzed; i.e., the global peak radial strain (GPRS), global peak circumferential strain (GPCS), global peak longitudinal stain (GPLS), and peak radial, circumferential, and longitudinal strain in each segment (PRS, PCS, and PLS, respectively). The LV ejection fraction (LVEF), LV end-diastolic volume, and LV end-systolic volume were quantified by delineating the endocardial and epicardial borders manually from the short axis.

Statistical analysis

Continuous variables are presented as mean ± standard deviation (SD). Categorical variables are presented as frequency and percentage. All data were controlled for a normal distribution by the Kolmogorov–Smirnov test and compared using the unpaired Student's t-test when normally distributed. Nonparametric tests were also applied for abnormally distributed data (Mann–Whitney U test). The association between the LVEF and LV strain parameters was assessed using Pearson correlation in all patients. Statistical analysis was performed with SPSS 22.0 (SPSS, Armonk, NY, USA). A P-value of <0.05 was regarded as statistically significant.

Results

Clinical characteristics

The clinical characteristics of the study population are shown in Table 1. Of 23 patients, 12 were male (52.5%). The average age was 50 years (range, 31–63 years). The healthy volunteers included 17 males (68%) with an average age of 27 years (range, 20–34 years). Compared with the control subjects, the cardiac function parameters (LVEF and stroke volume (SV)) were significantly decreased in DCM patients, while the LV end-diastolic volume and LV end-systolic volume were dramatically increased ($P < 0.001$).

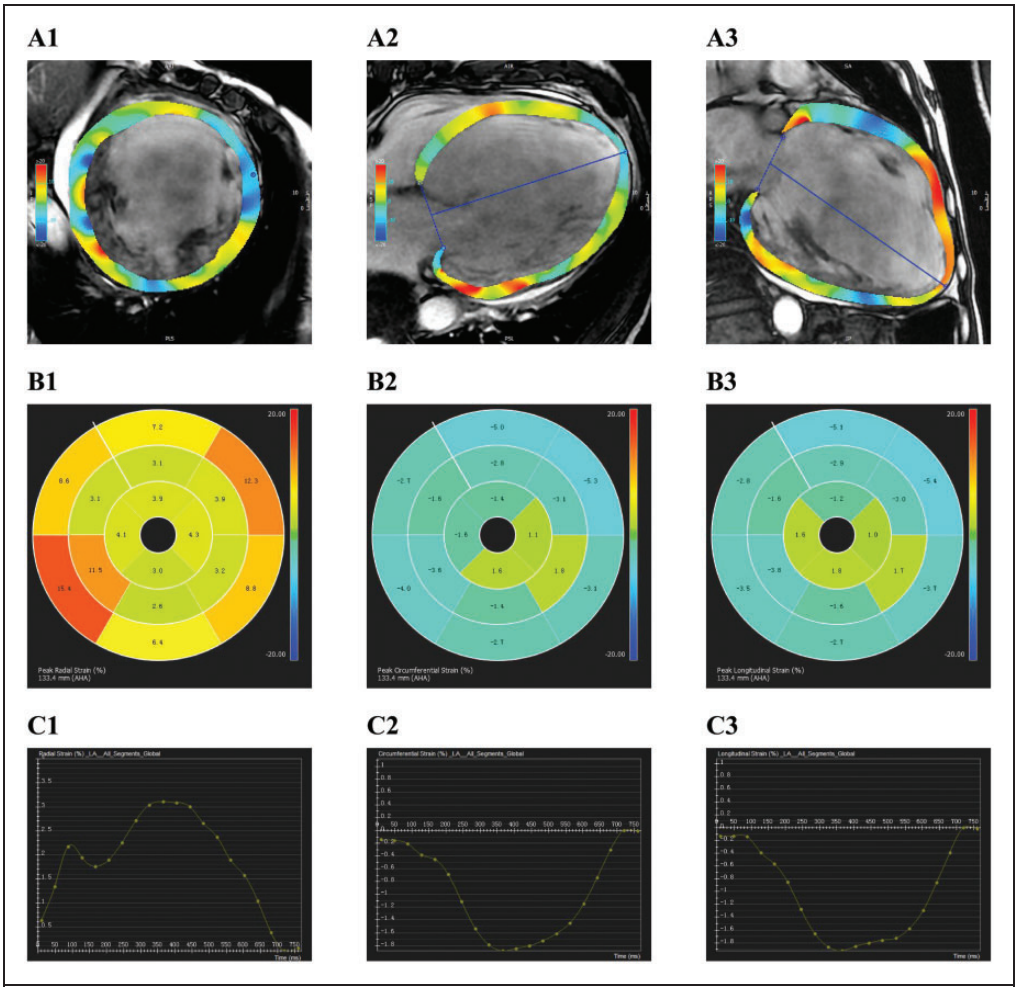

Figure 1. Representative example of the derivation of strain using cvi42 software in a 57-year-old patient with DCM. The result of LV tissue-tracking of cine steady-state free precession images in the axi, 2-ch, and 4-ch view. Picture A1–3: Myocardial pseudo-color map shows the strain values in the Axi, 4-ch, and 2-ch view. Picture B1–3: Strain of each segment on the bull's eye diagram of AHA for the peak radial strain (%), peak circumferential strain (%), and peak longitudinal strain (%), Picture C1–3: Global strain values. Red represents positive values, while blue represents negative; deeper colors indicate higher values.

The changes in the LVEF, SV, end-diastolic volume, and end-systolic volume indicated that the LV of patients with DCM was enlarged and that its contraction function was damaged, which is consistent with the pathological characteristics of DCM.[10]

Global strain analysis

As shown in Table 2, patients with DCM had a much lower global strain magnitude than control patients ($P < 0.001$). The GPRS was 8.60 ± 4.48 vs. 37.88 ± 7.50, the GPCS was -4.33 ± 1.86 vs. -14.38 ± 1.88, and the GPLS was -4.33 ± 1.76 vs. -11.85 ± 6.75.

Table 1. Baseline characteristics of patients with DCM and controls

Variable	DCM n = 23	Controls n = 25	*P* 值
Age (years)	50 ± 15	27 ± 6	<0.001
Sex (male)	12 (52.5%)	17 (68%)	–
LVEF (%)	22.42 ± 11.14	69.25 ± 6.75	<0.001
EDV (mL)	298.40 ± 128.82	133.60 ± 12.62	<0.001
ESV (mL)	248.80 ± 119.40	41.12 ± 11.69	<0.001
SV (mL)	62.07 ± 25.08	92.51 ± 17.25	<0.001

LVEF: left ventricular ejection fraction, EDV: end-diastolic volume, ESV: end-systolic volume, SV: stroke volume.

Table 2. Global strain of DCM and controls

Variable	DCM n = 23	Controls n = 25	*P* 值
GPRS	8.60 ± 4.48	37.88 ± 7.50	<0.001
GPCS	−4.33 ± 1.86	−14.38 ± 1.88	<0.001
GPLS	−4.33 ± 1.76	−11.85 ± 6.75	<0.001

GPRS: global peak radial strain, GPCS: global circumferential strain, GPLS: global peak longitudinal strain

We further studied the correlation between the LVEF and each of the global strains. As shown in Figure 2(a)–(c), a positive correlation was found between the GPRS and the LVEF ($R = 0.923$, $P < 0.01$), while the GPCS and GPLS were negatively correlated with the LVEF (GPCS: $R = -0.944$, $P < 0.01$; GPLS: $R = -0.895$, $P < 0.01$). Additionally, with pair-wise comparison, we also identified a negative correlation between the GPRS and GPCS as well as between the GPRS and GPLS, while the GPCS and GPLS were positively correlated with each other (Figure 2(d)–(f) (GPRS vs. GPCS: $R = -0.973$, $P < 0.01$; GPRS vs. GPLS, $R = -0.944$, $P < 0.01$; GPCS vs. GPLS, $R = 0.967$, $P < 0.01$).

Regional strain

The segmental values of the PRS, PCS, and PLS in normal subjects and patients with DCM are summarized in Table 3. We found that patients with DCM had significantly lower PRS, PCS, and PLS values at most segments to different degrees ($P < 0.05$); the only exception was the PCS at the apical septal segment and PLS at the apical anterior and inferior segments, where no significant difference could be identified ($P > 0.05$). Additionally, in all subjects, we found the PRS was highest in every segment, while the PLS was lowest.

Discussion

In this study, we used the latest technology (MR-TT) to analyze LV myocardial strains in patients with DCM, not only at a global strain level, but also at a regional strain level. Our results demonstrated that MR-TT is a promising method with which to detect early deregulated LV function in patients with DCM and guide clinical treatment of DCM.

We found that patients with DCM had a significantly reduced GPRS, GPCS, and GPLS, implying global LV impairment. The LV comprises two types of muscle bundles: longitudinal muscle bundles (including endocardial and epicardial fibers) and circumferential muscle bundles located in the midwall of the LV. The endocardial and epicardial fibers originate from the basal region, loop around the apex,

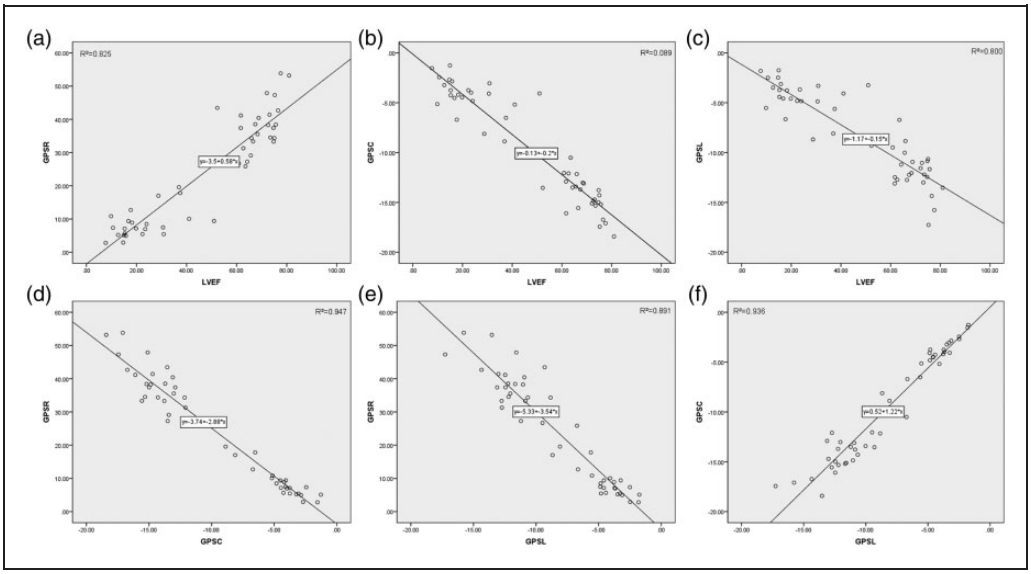

Figure 2. Relationship between the strain value and LVEF. (a–c) Association of LVEF and GPRS, GPCS, and GPLS ($R^2 = 0.85$, $R^2 = 0.89$, and $R^2 = 0.80$, respectively). (d–f) Linear correlations among GPRS, GPCS, and GPLS (GPRS vs. GPCS, $R^2 = 0.947$ $P < 0.01$; GPRS vs. GPLS, $R^2 = 0.891$, $P < 0.01$; GPCS vs. GPLS, $R^2 = 0.936$, $P < 0.01$). GPRS: global peak radial strain, GPCS: global circumferential strain, GPLS: global peak longitudinal strain.

and then return to the basal region, forming a helical structure.[11] When the LV becomes enlarged and spherical in patients with DCM, the longitudinal myocardium changes significantly; the longitudinal myocardial angle decreases and the muscle bundles change from longitudinal to horizontal. All of these changes can lower the subendocardial oxygen demand and increase the subendocardial blood flow, finally leading to reduced peak stains (GPRS, GPCS, and GPLS) in patients with DCM.[12] Moreover, we also found that the degree of damage was not same in each direction. GPRS changed more than GPCS and GPLS, indicating that patients with DCM had more serious damage in the radial direction of the LV. Additionally, the LV myocardium becomes thinner during the development of DCM, and the degree of thinning may vary in different places, further decreasing the PRS. Moreover, LV congestion leads to an increase in LV pressure, which induces heart movement resistance in the radial orientation and more obviously deceases radial strain. Although the LV myocardial movement was differentially reduced in patients with DCM, LV spherical expansion was obvious, which led to significant reduction of cardiac systolic function.

The LVEF is regarded as an important index with which to evaluate LV function. In this study, we found that the LV myocardial strains were significantly associated with the LVEF, which is consistent with previous reports.[13] The LVEF reflects the fractional change in the three-dimensional volume, and the strain determines the fractional change in the one-dimensional length from end-diastole to end-systole[14]; thus, these two measures are in parallel, which may lead to the significant association between the myocardial strain and the LVEF.

Table 3. Segmental values of strain in patients with DCM and controls

Variable	PRS		PCS		PLS	
Segment	Controls	DCM	Controls	DCM	Controls	DCM
Basal anterior	62.15 ± 17.93	8.55 ± 7.40*	− 20.49 ± 2.80	−9.24 ± 3.61*	−16.67 ± 4.80	−9.10 ± 3.31*
Basal anterior septal	25.67 ± 10.44	5.25 ± 5.70*	−12.89 ± 3.40	−5.78 ± 3.19*	−15.71 ± 4.98	−6.37 ± 3.28*
Basal interior septal	21.44 ± 9.80	6.92 ± 7.48*	−12.84 ± 3.60	−4.24 ± 2.77*	−15.57 ± 4.90	−4.26 ± 3.93*
Basal inferior	32.13 ± 10.85	10.40 ± 10.16*	−14.80 ± 3.26	−3.67 ± 4.54*	−15.15 ± 4.93	−5.82 ± 3.16*
Basal inferior lateral	45.90 ± 14.70	15.48 ± 9.68*	−19.24 ± 3.3	−6.49 ± 3.98*	−15.98 ± 5.50	−7.97 ± 3.08*
Basal anterior lateral	60.57 ± 21.24	15.21 ± 13.06*	−22.23 ± 3.79	−9.25 ± 3.74*	−17.31 ± 5.20	−9.49 ± −9.49*
Middle anterior	47.54 ± 19.02	8.40 ± 6.62*	−20.04 ± 3.21	−7.35 ± 3.89*	−20.96 ± 3.11	−7.62 ± 4.05*
Middle anterior septal	26.96 ± 9.28	9.06 ± 5.54*	−10.82 ± 6.39	−6.46 ± 4.28‡	−9.80 ± 6.74	−6.27 ± 4.13‡
Middle inferior	23.25 ± 3.95	9.32 ± 7.97*	−12.28 ± 8.17	−4.83 ± 4.80*	−11.04 ± 7.86	−3.74 ± 4.97*
Middle inferior	33.48 ± 8.22	5.07 ± 6.13*	−18.46 ± 3.20	−0.19 ± 5.89*	−16.96 ± 2.96	−054 ± 5.50*
Middle inferior lateral	40.90 ± 14.93	7.45 ± 6.53*	−23.37 ± 4.63	−2.36 ± 5.73*	−22.45 ± 4.45	−3.52 ± 5.17*
Middle anterior lateral	39.91 ± 12.89	11.23 ± 8.44*	−22.73 ± 4.71	−7.06 ± 5.26*	−23.05 ± 4.86	−7.84 ± 4.90*
Apical anterior	51.88 ± 20.57	15.34 ± 8.94*	−9.65 ± 2.98	−4.07 ± 2.10*	−1.53 ± 6.32	−2.32 ± 2.18
Apical septal	39.89 ± 11.63	12.03 ± 6.82*	−2.41 ± 8.77	−3.29 ± 3.83	5.05 ± 4.60	−1.49 ± 3.59*
Apical inferior	49.98 ± 19.93	6.96 ± 8.33*	−12.33 ± 5.31	2.06 ± 4.03*	−0.32 ± 7.63	2.65 ± 2.88
Apical lateral	59.82 ± 20.98	14.98 ± 11.10*	−17.13 ± 5.53	−0.33 ± 4.87*	−7.01 ± 7.07	1.01 ± 4.16*

*$P < 0.001$, ‡$P < 0.05$.

To the best of our knowledge, the present study is the first to analyze the correlations among the PRS, PCS, and PLS. A previous study showed that the PCS had a linear correlation with the PLS ($R = 0.82$, $P < 0.05$) using three-dimensional speckle-tracking echocardiography.[15] In the present study, we performed pair-wise comparison among the PRS, PCS, and PLS, which showed linear correlations among one another (figure 2). The results indicated that the generation of LV myocardial strain was not isolated but integrated. In other words, LV wall motion depends on teamwork between the longitudinal and circumferential muscle bundles from all directions.

Additionally, with respect to the segmental myocardial strains, we found that the PRS, PCS, and PLS were significantly reduced in most LV myocardial segments, but the magnitudes of different strains were largely different from each other. This is consistent with the fact that DCM is characterized by diffuse progression throughout the whole heart; however, the degree of damage was heterogeneous. Regardless, we did not identify an obvious difference in the apical anterior and inferior segments of PLS, which might have been due the more complex and unstable movement of the apex.[16]

A few limitations of this study should be kept in mind. First, the large SD of the peak strains, which in the normal population is similar to that reported with other methodologies,[7] was also mentioned in the study by Taylor et al.,[17] who used CMR feature-tracking. In the present study, the SD of the peak strain in DCM was higher than that in the normal population because the myocardial motion was unstable, indicating LV myocardial dysfunction in patients with DCM. Second, the number of patients with DCM was relatively small; consequently, our results must be confirmed by a further study involving a larger sample size. Third, the patients with DCM and normal volunteers were not matched for age, which may have affected the results of the study; previous studies have found that increased age would cause the PCS to change. Finally, MR-TT is an emerging technology, and it remains to be validated in clinical studies.

Declaration of Conflicting Interest

The author(s) declared no potential conflicts of interest with respect to the research, authorship, and/or publication of this article.

Funding

The author(s) disclosed receipt of the following financial support for the research, authorship, and/or publication of this article: This work was supported by the National Natural Science Foundation of China (Grant Nos. 81360216 and 81660284), the Major Program of the Natural Science Foundation of Jiangxi, China (Grant No. 20161ACB20013), and the Key Program of the Bureau of Science & Technology of Jiangxi Province (Grant No. 20121BBG70040).

References

1. Rakar S, Sinagra G, Di Lenarda A, et al. Epidemiology of dilated cardiomyopathy. A prospective post-mortem study of 5252 necropsies. The heart muscle disease study group. *Eur Heart J* 1997; 18: 117–123.
2. Jefferies JL and Towbin JA. Dilated cardiomyopathy. *Lancet* 2010; 375: 752–762.
3. Osman NF and Prince JL. Visualizing myocardial function using HARP MRI. *Phys Med Biol* 2000; 45: 1665–1682.
4. Hor KN, Gottliebson WM, Carson C, et al. Comparison of magnetic resonance feature tracking for strain calculation with harmonic phase imaging analysis. *JACC Cardiovasc Imaging* 2010; 3: 144–151.
5. Sitia S, Tomasoni L and Turiel M. Speckle tracking echocardiography: a new approach to myocardial function. *World J Cardiol* 2010; 2: 1–5.

6. Pennell DJ. Cardiovascular magnetic resonance. *Circulation* 2010; 121: 692–705.
7. Schuster A, Stahnke VC, Unterberg-Buchwald C, et al. Cardiovascular magnetic resonance feature-tracking assessment of myocardial mechanics: Intervendor agreement and considerations regarding reproducibility. *Clin Radiol* 2015; 70: 989–998.
8. Obokata M, Nagata Y, Wu VC, et al. Direct comparison of cardiac magnetic resonance feature tracking and 2D/3D echocardiography speckle tracking for evaluation of global left ventricular strain. *Eur Heart J Cardiovasc Imaging* 2016; 17: 525–532.
9. Richardson P, McKenna W, Bristow M, et al. Report of the 1995 World Health Organization/International Society and federation of cardiology task force on the definition and classification of cardiomyopathies. *Circulation* 1996; 93: 841–842.
10. Mann DL and Bristow MR. Mechanisms and models in heart failure: the biomechanical model and beyond. *Circulation* 2005; 111: 2837–2849.
11. Anderson RH, Ho SY, Redmann K, et al. The anatomical arrangement of the myocardial cells making up the ventricular mass. *Eur J Cardiothorac Surg* 2005; 28: 517–525.
12. Beyar R and Sideman S. The dynamic twisting of the left ventricle: a computer study. *Ann Biomed Eng* 1986; 14: 547–562.
13. Cheng-Baron J, Chow K, Pagano JJ, et al. Quantification of circumferential, longitudinal, and radial global fractional shortening using steady-state free precession cines: a comparison with tissue-tracking strain and application in Fabry disease. *Magn Reson Med* 2015; 73: 586–596.
14. Parisi AF, Moynihan PF, Feldman CL, et al. Approaches to determination of left ventricular volume and ejection fraction by real-time two-dimensional echocardiography. *Clin Cardiol* 1979; 2: 257–263.
15. Maciver DH. The relative impact of circumferential and longitudinal shortening on left ventricular ejection fraction and stroke volume. *Exp Clin Cardiol* 2012; 17: 5–11.
16. Matsumoto K, Tanaka H, Tatsumi K, et al. Left ventricular dyssynchrony using three-dimensional speckle-tracking imaging as a determinant of torsional mechanics in patients with idiopathic dilated cardiomyopathy. *Am J Cardiol* 2012; 109: 1197–1205.
17. Taylor RJ, Moody WE, Umar F, et al. Myocardial strain measurement with feature-tracking cardiovascular magnetic resonance: normal values. *Eur Heart J Cardiovasc Imaging* 2015; 16: 871–881.